Title

Parallel RNA Interference Screens Identify EGFR Activation as an Escape Mechanism in FGFR3-Mutant Cancer

Journal

Cancer Discovery, 3(9)

ISSN

2159-8274

Authors

Herrera-Abreu, Maria Teresa
Pearson, Alex
Campbell, James
et al.

Publication Date

2013-09-01

DOI

10.1158/2159-8290.cd-12-0569

Peer reviewed

Published in final edited form as:
Cancer Discov. 2013 September ; 3(9): 1058–1071. doi:10.1158/2159-8290.CD-12-0569.

Parallel RNA interference screens identify EGFR activation as an escape mechanism in *FGFR3* mutant cancer

Maria Teresa Herrera-Abreu[1], **Alex Pearson**[1], **James Campbell**[1], **Steve D Shnyder**[2], **Margaret A Knowles**[3], **Alan Ashworth**[1], and **Nicholas C Turner**[1,4]

[1]The Breakthrough Breast Cancer Research Centre, Institute of Cancer Research, London, SW3 6JB, UK.

[2]Institute of Cancer Therapeutics, University of Bradford, Richmond Road, Bradford BD7 1DP, UK

[3]Section of Experimental Oncology, Leeds Institute of Molecular Medicine, St James's University Hospital, Leeds, LS9 7TF, UK

[4]Breast Unit, Royal Marsden Hospital, Fulham Road, London, SW3 6JJ, UK

Abstract

Activation of fibroblast growth factor receptors is a common oncogenic event. Little is known about the determinants of sensitivity to FGFR inhibition and how these may vary between different oncogenic FGFRs. Using parallel RNA interference genetic screens we demonstrate that EGFR limits sensitivity to FGFR inhibition in *FGFR3* mutant and translocated cell lines, but not in other *FGFR* driven cell lines. We also identify two distinct mechanisms through which EGFR limits sensitivity. In partially FGFR3 dependent lines, inhibition of FGFR3 results in transient down-regulation of MAPK signalling that is rescued by rapid upregulation of EGFR signalling. In cell lines that are intrinsically resistant to FGFR inhibition, EGFR dominates signalling via repression of FGFR3, with EGFR inhibition rescued by delayed up-regulation of FGFR3 expression. Importantly, combinations of FGFR and EGFR inhibitors overcome these resistance mechanisms *in vitro* and *in vivo*. Our results illustrate the power of parallel RNA interference screens in identifying common resistance mechanisms to targeted therapies.

Keywords

FGFR3; EGFR; siRNA screen; Bladder cancer

Introduction

Activating mutations of the FGF receptors are found in multiple cancer types, with the highest prevalence occurring with *FGFR3* mutations in bladder cancer (1) and *FGFR2* mutations in endometrial cancer (2, 3). In other cancer types activation of FGFR receptors occurs predominantly through receptor gene amplification, with *FGFR1* amplification in squamous lung and breast cancer(4, 5), and *FGFR2* amplification in gastric and breast cancers(6, 7). Further mechanisms of activation include activating translocations involving

Corresponding author: **Nicholas Turner,** The Institute of Cancer Research, 237 Fulham Road, London, SW3 6JB, UK, Fax: +44 (0) 207 51535340, nicholas.turner@icr.ac.uk.

Conflict of interest: We have no conflicts of interest

Europe PMC Funders Author Manuscripts

the FGFRs, described initially in haematological malignancies although recently also described in solid tumours (8, 9) and FGF ligand mediated signalling (10).

Preclinical studies have suggested that activated FGF receptors are potential therapeutic targets (2, 3, 6, 11-13), and multiple FGF receptors inhibitors have entered clinical trial with early evidence of efficacy with FGFR inhibitors in *FGFR1* amplified breast cancer and lung cancer (14, 15). Yet it is not clear what determines whether cancers will respond to FGFR inhibitors, what the mechanisms of resistance will be, and how this may vary between different oncogenic receptors and cancer types. This presents a major limitation to the clinical development of FGFR inhibitors, as it is unclear which of the diverse mechanisms of activation of the FGF receptors are most likely to translate to clinical efficacy.

RNA interference (RNAi) screens have substantial potential in elucidating the determinants of sensitivity to cancer therapies (16-18), identifying both mechanisms of resistance (17) and key pathways that determine sensitivity (18). Here, we use parallel short interfering RNA (siRNA) screens to identify determinants of sensitivity and mechanisms of resistance to FGFR inhibition in the protein kinome/phosphatome, along with a panel of amplified and mutant cancer cell lines to identify mechanisms specific to different *FGFR* mutation and amplifications. Through this approach we identify EGFR as a major factor limiting the efficacy of targeting *FGFR3* mutations.

Results

High-throughput Kinome/Phosphatome screens

To identify the determinants of sensitivity to FGFR inhibitors we conducted high-throughput parallel siRNA screens using a library targeting all known protein kinases and phosphatases in a panel of 11 *FGFR* amplified, mutant or translocated cell lines (Figure 1A). Such parallel siRNA screens allow for comparison between different oncogenic aberrations, and have the potential to identify key mutation or subtype specific mechanisms of resistance. The screening panel represented the most common *FGFR* aberrations observed in carcinomas, including cell lines with *FGFR1* amplification (JMSU1, H1581), *FGFR2* amplification (MFM223, SUM52, SNU16, KATOIII, OCUM2M), *FGFR2* mutation (AN3CA), and *FGFR3* activated (*FGFR3* point mutated 97-7 and MGHU3, and RT112M that has an activating *FGFR3-TACC3* fusion) (Supplementary Table 1). Cell lines were transfected with the siRNA library in triplicate, and 48 hours later half of the plates were treated with the cell line EC50 dose of the pan-FGFR inhibitor PD173074 and half with vehicle for 72 hours (Figure 1A and 1C). Vehicle control plates were used to examine for the effect of siRNA on cell survival/growth, and the relative growth in plates exposed to PD173074 versus vehicle was used to identify siRNA that altered sensitivity to PD173074 (Figure 1A).

Across the panel of *FGFR* driven cell lines, *FGFR1* amplified cell lines and *FGFR2* amplified/mutated cell lines were selectively sensitive to the corresponding siRNA, (Figure 1B), with in particular *FGFR2* amplified cell lines being strongly addicted to FGFR2. Similarly, across the panel of cell lines silencing of FGFR1 or FGFR2 was epistatic to FGFR inhibition in the corresponding cell lines (Supplementary Figure 1A). Unexpectedly a similar effect was not seen with FGFR3 siRNA in the *FGFR3* activated cell lines, with FGFR3 siRNA having little or no effect on cell survival (Figure 1B). *FGFR3* cell lines were also noted to be relatively insensitive to PD173074 (Figure 1C), potentially suggesting the existence of alternative drivers of proliferation in the *FGFR3* activated cell lines, and here we focus on identifying the alternative drivers and mechanisms of resistance in these cell lines.

EGFR is a key mediator of resistance in FGFR3 activated cell lines

We set out to identify what determined sensitivity in *FGFR3* activated cell lines and the factors that limited the sensitivity of these cell lines to FGFR inhibition. To identify features common to all three *FGFR3* activated cell lines we performed supervised hierarchical clustering to identify the siRNA that differentially modulated sensitivity to PD173074 in *FGFR3* activated cell lines compared to the other *FGFR* driven cell lines (Figure 1D). EGFR siRNA was the top siRNA that differentially increased sensitivity to PD173074 in the *FGFR3* activated cell lines (Figure 1D). This illustrated the potential power of parallel siRNA screens to identify common subgroup specific resistance mechanism, as EGFR siRNA was obscured by a multiplicity of effects and noise in individual screens (Supplementary Figure 1B). A number of additional hits identified were potentially linked to EGFR signalling in network analysis (Supplementary Figure 1C). EGFR siRNA sensitised all three of the *FGFR3* activated bladder cell lines screened to PD173074, but none of the other cell lines, identifying a clear subtype/mutation specific event (Figure 1E). EGFR siRNA also reduced the survival of the PD173074 insensitive 97-7 cell line, suggesting that this cell line may be primarily EGFR dependent (Figure 1E).

The effect of silencing EGFR on sensitivity to PD173074 was validated with two independent siRNA targeting EGFR (Figure 2A and 2B), and the selectivity of the effect to *FGFR3* activated cell lines was also confirmed with EGFR inhibitors (lapatinib and gefitinib) in short term survival assays (Supplementary Figure 2A). To understand why EGFR siRNA appeared to sensitise only *FGFR3* activated cell lines, we examined EGFR expression and phosphorylation by western blotting. The *FGFR3* activated bladder cancer cell lines expressed high levels of both total and phosphorylated EGFR (Figure 2C), with EGFR either not expressed or phosphorylated in the other cell lines. This suggested that the specificity of the effect seen with EGFR siRNA (Figure 1E) in part reflected expression and intrinsic activation of EGFR in the *FGFR3* cell lines. In the blots FGFR3 was expressed at a number of different molecular weights (Figure 2C). RT112M are driven by an *FGFR3-TACC3* fusion of higher molecular weight than wild-type FGFR3. FGFR3 is expressed as two forms, a lower molecular weight unglycosylated form and a higher molecular weight glycosylated form indicated by arrows, with in particular the glycosylated form expressed at low level in 97-7 (Figure 2C).

We performed clonogenic assays in the *FGFR3* activated cell lines to further examine the potential role of EGFR in these cell lines. Colony formation was either abolished, or substantially decreased, by the combination of PD173074 and gefitinib (Figure 2D). To confirm that this observation extended beyond the cell lines used in the screen, we treated additional *FGFR3* point mutant cell lines, again with substantial combination efficacy in 94-10 and 639V (Figure 2D). Similar synergy was also seen between the clinical FGFR inhibitor AZD4547 and geftinib, or cetuximab and PD173074 in the RT112M cell line (Supplementary Figure 2C and 2D).

Two distinct patterns of response to PD173074 and gefitinib were apparent in the clonogenic and short-term survival assays (Figure 2D, Figure 1C and Supplementary Figure 2A and B). The RT112M, MGHU3, and 639V cell lines were partially FGFR dependent: PD173074 modestly reduced colony formation although combination with the EGFR inhibitor gefitinib further reduced clonogenic survival, suggesting that in these cell lines EGFR limited sensitivity to FGFR inhibition. In contrast, the 97-7 and 94-10 cell lines were principally EGFR dependent: Gefitinib alone susbstantially reduced colony formation with PD173074 alone having no effect on the growth of these cell lines, suggesting that EGFR mediated the intrinsic resistance of these cell lines to PD170374. In the presence of gefitinib, clonogenic survival was further reduced by PD173074, suggesting that reciprocally in 97.7 and 94.10 FGFR signalling limited the sensitivity to EGFR inhibition.

In both 97-7 and RT112M combined inhibition of FGFR and EGFR, with PD173074 and gefitinib, induced a greater loss of S phase compared to either inhibitor given alone (Figure 2E and Supplementary Figure 3A), concomitant with a relatively increased p27 levels with the combination (Figure 2F). Gefitinib, and in particular the combination, increased PARP cleavage in 97-7 (Figure 2F) although with only a relatively minor increase in Annexin V staining was observed (Supplementary Figure 3B). This suggested that the combined effect of the inhibitors was mediated predominantly through greater cell cycle arrest, along with a minor increase in apoptosis.

Inhibition of FGFR3 results in upregulation of EGFR signalling in partially FGFR3 dependent cell lines

We identified that EGFR signalling limited sensitivity to FGFR3 targeting in all five *FGFR3* activated cell lines examined. We described two groups of *FGFR3* activated cell lines: one group partially *FGFR3* dependent with EGFR signalling limiting sensitivity to FGFR inhibitors; and the other group primarily EGFR dependent with intrinsic resistance to FGFR inhibitors, although in these cell lines FGFR signalling limited sensitivity to EGFR inhibition. We investigated the link between EGFR and FGFR3 signalling in these cell lines, how one receptor compensated for inhibition of the alternative receptor, and whether the same mechanisms where involved in the partially FGFR3 dependent and EGFR dependent cell lines.

We first focused on the cell lines that were partially FGFR3 dependent. In the RT112M and 639V cell lines PD173074 completely suppressed ERK1/2 phosphorylation at 1 hour, confirming the FGFR3 was the dominant receptor in these cell lines (Figures 3A). However, at later time points ERK1/2 phosphorylation was partially restored, reaching steady state by 4 hours. The increase in ERK1/2 phosphorylation was accompanied by upregulated EGFR Tyr1068 phosphorylation (Figure 3A). A similar pattern was also seen in the PD173074 sensitive MGHU3 cell line (Supplementary Figure 4A). The restoration of ERK1/2 phosphorylation was blocked by the addition of gefitinib both at 6 hours and chronically at 24 hours (Figure 3B), and the combination of PD173074 with gefitinib lead to greater suppression of AKT-Ser473 phosphorylation in RT112M than was seen with PD173074 alone (Figure 3C). To ascertain whether the reactivation of MAPK signalling explained the relative insensitivity to FGFR inhibition, we examined the combination of PD173074 and the MEK inhibitor CI-1040. In RT-112M cells, CI-1040 increased sensitivity to PD170374 in clonogenic assays suggesting that in part reactivation of MEK-ERK1/2 signalling by EGFR reduced sensitivity to PD173074 (Figure 3D).

Mechanism of EGFR activation by FGFR inhibitors

We set out to establish how EGFR gets activated and subsequently upregulated by FGFR3 inhibition. EGFR was wild-type in all five *FGFR3* activated cell lines and the *EGFR* gene was not amplified (data not shown). The *FGFR3* activated bladder cancer cell lines expressed high levels of TGFα with silencing of TGFα in RT112M increasing sensitivity to PD173074 suggesting an autocrine loop (Supplementary Figure 4B). There was no change in the expression of TGFα in response to PD173074 (Supplementary Figure 4C), suggesting that upregulation of EGFR signalling in response to PD173074 did not reflect increased TGFα ligand expression. We were also unable to demonstrate co-immunoprecipitation between EGFR and FGFR3 suggesting that the two receptors did not interact (Supplementary Figure 4D).

In the EGFR dependent cell lines 97-7 and 94-10, PD170374 had no effect on down-stream signalling and no effect of EGFR phosphorylation (Figure 3A), suggesting that the upregulation of EGFR seen with PD173074 in FGFR3 dependent cell lines did not reflect

FGFR inhibition *per se*, but the resulting loss of down stream signalling. We hypothesised that the decrease in ERK1/2 activity that occurred with PD173074, resulted in the upregulation of EGFR signalling, and inhibition of MEK with CI-1040 in RT112M cells decreased ERK1/2 phosphorylation and substantially upregulated EGFR Tyr1068 phosphorylation (Figure 3E). This therefore suggested a model whereby FGFR3 mediated MAPK signalling suppressed signalling from EGFR, and that this negative feedback was subsequently released by FGFR3 inhibition.

Multiple mechanisms of regulation of EGFR signalling through negative feedback loops mediated by MEK-ERK1/2 signalling have been described, such as the ERK1/2 mediated phosphorylation of CBL to promote receptor internalisation and degradation, and to promote expression of the sprouty proteins (19). In addition the CDC25 familly has been identified as a potential EGFR phosphatases (20) that have previously been suggested to mediate a feedback loop between inhibition of mutant *BRAF*, loss of MEK-ERK1/2 signalling, and upregulation of EGFR (17, 21). Silencing CDC25C with multiple different siRNA increased EGFR phosphorylation and downstream signalling (Supplementary Figure 4E). However, we were unable to demonstrate a decrease in CDC25C-Thr48 phosphorylation with PD170374 in RT112M cells, the site proposed to be regulated by ERK1/2 (21) (Supplementary Figure 4F), suggesting that although CDC25C is a phosphatase that regulates EGFR phosphorylation and signalling, it was unlikely to be involved in the feedback upregulation mediated by PD173074 in these cell lines. Moreover, the siRNA against CDC25C did not affect sensitivity to PD173074 in either RT112M or MGHU3 (Supplementary Figure 4G).

Receptor internalisation and trafficking is a major factor regulating the signalling from receptor tyrosine kinases, with internalisation ultimately leading to signal termination (19). After internalisation, EGFR continues to signal from early endosomes with signalling only terminated later due to subsequent lysosomal degradation, or in late recycling endosomes (19). Silencing of CBL with multiple different siRNA decreased sensitivity to PD173074 (Supplementary Figure 4H), potentially suggesting a role for receptor trafficking in sensitivity to PD173074. To examine if there was a defect in receptor trafficking that may contribute to EGFR upregulation we examined EGFR location by immunofluorescence. In RT112M cells, PD173074 treatment led to EGFR accumulating at the plasma membrane (Figure 4A and B), in regions characterised by aberrant dense cortical filamentous actin (F-actin) (Figure 4A). EGFR also accumulated in giant actin coated rings (Figure 4C) that stained with EEA1 (Figure 4D), indicating accumulation of EGFR in giant early endosomes (Figure 4C and D). These results suggested that the activation of EGFR following FGFR was mediated by both loss of ERK1/2 induced negative feedback, and impaired receptor internalisation and sorting that would contribute through impaired signalling termination.

EGFR mediates intrinsic resistance to FGFR3 targeting through repression of FGFR3 expression

We next focused on the cell lines that were primarily EGFR dependent, to understand why these cell lines were EGFR dependent and intrinsically resistance to FGFR targeting (Figure 2D and supplementary Figure 2A and B). Both of the EGFR dependent cell lines, 97-7 and 94-10, had a S249C *FGFR3* activating mutation identical to germline *FGFR3* activating mutations found in a proportion of people with the skeletal dysplasia syndrome thanatophoric dysplasia (22, 23). S249C constitutively activates the kinase through constitutive receptor dimerisation as a result of an aberrant extracellular inter-molecular disulphide bridge (22, 24). Expression of the *FGFR3* mutation was confirmed by RT-PCR (Supplementary Figure 5A). In the EGFR dependent cell lines 97-7 and 94-10 gefitinib acutely blocked both ERK1/2 and AKT-Ser473 phosphorylation confirming that EGFR dominated down stream signalling in these cell lines and not the mutant FGFR3 receptor

(Figure 5A). Gefitinib alone had no effect on signalling in the FGFR3 dependent cell lines (Figure 5A), an inverse of the effect seen with PD173074 (Figure 3A). Therefore, in any one cell line either FGFR3 or EGFR was the dominant receptor controlling signalling, and this directly reflected the sensitivity to the corresponding inhibitor.

Whereas in the FGFR3 dependent cell lines PD173074 lead to relatively rapid upregulation of EGFR and restoration of ERK1/2 phosphorylation (Figure 3), in the EGFR dependent cell lines the restoration of ERK1/2 phosphorylation was much delayed only occuring after 24 hours exposure to gefitinib (Figure 5A). The delayed restoration of ERK1/2 phosphorylation was blocked by PD173074, both at 24 hours and 48 hours after gefitinib addition (Figure 5B and 5C), confirming that in these cell lines FGFR signalling compensated for the loss of EGFR signalling. The very substantial difference in the kinetics of the restoration of downstream signalling by the non-dominant EGFR or FGFR3 receptor (Figure 3A and 5A) suggested that the mechanism(s) leading to upregulation of FGFR3 signalling were distinct. Concurrent with the increase in ERK1/2 phosphorylation we observed substantial upregulation of FGFR3 protein, in particular the fully glycosylated form (Figure 5A), with consequent upregulation of FRS2 phosphorylation (adapter protein of FGFRs, Figure 5D).

To confirm that EGFR signalling could repress FGFR3 expression, we hyper-activated EGFR in the partially FGFR3 dependent cell line RT112M. Supplementation of media with TGFα resulted in RT112M becoming resistant to PD173074 (Figure 5E) accompanied by near complete repression of FGFR3-TACC3 expression (Figure 5F). In the EGFR dominant cell lines, compared to cell lines where FGFR3 signalling dominated, EGFR was expressed at substantially higher levels relative to FGFR3 (Figure 2C, and Figure 5G and 5H), and similarly EGFR was phosphorylated at substantially higher levels in 97-7 compared to RT112M or MGHU3 (Figure 2C). This suggested that the relative expression and activation level of EGFR may have dictated whether the cell line became EGFR dependent.

To investigate how EGFR signalling led to repression of FGFR3 we first examined *FGFR3* mRNA expression. Gefitinib lead to substantial increased *FGFR3* mRNA levels in the EGFR dependent 97-7 cell line (Figure 6A), with the increase in mRNA seen not at 6 hours but at 24 hours mirroring the timing of increased FGFR3 protein (Figure 5A). We examined which signalling pathways down-stream of EGFR might regulate *FGFR3* mRNA expression, treating 97-7 with a panel of signal transduction inhibitors (Figure 6B). Inhibition of PI3 kinase with GDC0941, or AKT with AZD5363, did not result in upregulation of *FGFR3* mRNA (Figure 6B) nor FGFR3 protein (Figure 6C). Inhibition of AKT-Ser473 phosphorylation by GDC0941, and stimulation by AZD5363, confirmed target inhibition by the respective inhibitors. Therefore, although PI3K / AKT inhibition results in upregulation of multiple receptor tyrosine kinases, for example of the EGFR/ERBB family (25, 26), PI3K / AKT signalling alone did not repress *FGFR3* expression. Similarly solitary inhibition of MEK, JAK2, PKCα/β, or ROCK had no effect, or further repressed, *FGFR3* mRNA expression (Figure 6B).

Across the panel dasatinib, utilized at 100nM that is relatively specific to the SRC family of kinases along with ABL/KIT (27), resulted in clear *FGFR3* mRNA upregulation (Figure 6B) along with upregulated FGFR3 protein (Figure 6D). Hyper-activation of EGFR with TGFα in RT112M, that repressed FGFR3 expression, also resulted in substantial SRC-Tyr416 phosphorylation (Figure 5F). SRC signalling has previously been suggested to regulate FGFR3 expression by regulation of microRNA miR-99a (28). However, RT112M have an *FGFR3-TACC3* translocation that removes the 3′UTR and is consequently not targeted by miR-99a (29), or other FGFR3 regulatory microRNA, implying that the repression of FGFR3 was not due to the effects of microRNA (Figure 5F). Similarly, transfection of microRNA inhibitors against miR-99a and miR-100 in 97-7 cells, microRNA that have been

Europe PMC Funders Author Manuscripts

shown to regulate FGFR3 expression in bladder cancer (30), did not alter FGFR3 expression (Supplementary Figure 5B).

EGFR and SRC interact, cross-phosphorylate each other, and mutually reinforce down-stream signalling (31, 32). As we were unable to demonstrate that inhibition of a single down-stream signal transduction pathway repressed FGFR3 expression (Figure 6B) we examined combination pathway inhibition. Combined inhibition of MEK and PI3 kinases resulted in substantial de-repression of FGFR3 (Figure 6E), suggesting that EGFR signalling reinforced by SRC repressed FGFR3 expression through the combined action of multiple down-stream pathways. Therefore, these data suggest that EGFR signalling repressed *FGFR3* transcription, and gefitinib released this repression resulting in restoration of FGFR3 expression and signalling. Similar to that observed with EGFR, FGFR3 also accumulated in the cytoplasmic membrane after gefitinib treatment (Figure 6F and Supplementary Figure 5C), whereas in untreated cells FGFR3 was predominantly cytoplasmic, suggesting that upregulation of FGFR3 was also reinforced by impaired receptor internalisation.

In vivo efficacy of combined EGFR and FGFR inhibition

To investigate efficacy *in vivo*, we established xenografts of RT112M cells in nude mice. The combination of gefitinib and PD173074 was poorly tolerated at the doses used with rapid weight loss (Supplementary Figure 6A). Nevertheless, the short duration of 3 days combination therapy reduced tumour volume to a greater extent than either treatment given alone, including two complete responses (Figure 7A), confirming that the *in vitro* observations predicted for greater tumour control with combination treatment *in vivo.*

We repeated experiments with the combination of cetuximab and PD173074 given for two weeks of treatment, which was well tolerated (Supplementary Figure 6B). The combination of cetuximab and PD173074 reduced tumour size to a significantly greater extent than either agent given alone ($p<0.0001$ Log-Rank test, Figure 7B). Treatment with PD173074 leads to tumour stasis whereas combination therapy leads to substantial tumour reduction (mean relative tumour volume at end of 2 week treatment period 1.28 PD173074 vs. 0.51 combination, $p=0.006$ Student's T-test). On stopping treatment PD173074 tumours rapidly resumed growth, whereas the combination treated animals had sustained tumour control (median time to tumour doubling control 6 days, cetuximab 13 days, PD173074 17 days, combination group median not reached after 41 days follow-up, Figure 7C). These dated suggested substantial synergistic efficacy *in vivo* between dual targeting of EGFR and FGFR3 in *FGFR3* activated cell lines.

Discussion

In this study we have utilized parallel RNA interference screens in multiple FGFR dependent cell lines to dissect mechanisms of resistance to FGFR inhibition. We show that the sensitivity of *FGFR3* activated cancers is limited by intrinsic activation of EGFR in all the cell lines studied, and we described two distinct mechanistic groups. In partially FGFR3 dependent cell lines, EGFR signalling is upregulated following FGFR inhibition through release from negative feedback, and this partially compensates for loss of FGFR signalling. In EGFR dependent cell lines, despite the presence of an activating *FGFR3* mutation, EGFR dominates down-stream signalling through repression of FGFR3 expression. In the EGFR dependent cell lines, EGFR inhibition resulted in delayed upregulated FGFR3 expression, restoring FGFR3 signalling and partially compensating for loss of EGFR signalling.

We demonstrate a reciprocal relationship between targeting the dominant oncogene and rescue mediated by an alternative receptor tyrosine kinase, which is emerging as a major mechanism of resistance to cancer therapies (33-36). In FGFR3 dependent cell lines, EGFR

signalling is upregulated relatively rapidly following loss of MAPK signalling negative feedback induced by PD173074 (Figure 3E). FGFR inhibition in *FGFR3* activated cell lines did not induce an apoptotic response (Figure 2F and Supplementary Figure 3), and potentially such a cytostatic response allows for upregulation of the alternative receptor to subvert the effect of inhibition of the dominant receptor. In contrast, in EGFR dependent cell lines rescue from EGFR inhibition is reliant on delayed de-repression of FGFR3 expression. Impaired receptor trafficking re-inforces the upregulation of both receptors. In response to FGFR3 inhibition, EGFR accumulates at the membrane and in early endosomes, and likewise in response to EGFR inhibition FGFR3 accumulates at the membrane. FGFR3 and EGFR were noted to accumulate at the membrane in areas of abnormally dense actin filament formation, and it will be interesting in future research to examine the possible role of aberrant regulation of the cytoskeleton in receptor accumulation (37).

EGFR dominates down stream signalling in some *FGFR3* mutant cell lines through repression of mutant FGFR3 expression resulting in intrinsic resistance to FGFR inhibitors. Although *FGFR3* mutation presumably initiated cancer development in these cancers, at some point in tumour development EGFR signalling rose to a level where it repressed mutant FGFR3 and dominated down-stream signalling. Whereas prior research has emphasised the role of PI3 kinase – AKT signalling in repression of receptor tyrosine kinases (25, 26), neither inhibition of PI3 kinase nor AKT alone de-repressed FGFR3 expression in the EGFR dominant cell lines (Figure 6B/C). In contrast inhibition of SRC family kinases with dasatinib resulted in substantial FGFR3 de-repression. Whereas EGFR signals strongly to SRC (Figure 5F), mutant *FGFR3* has been shown to signal only weakly to SRC (24), and the difference in down-stream signalling between EGFR and mutant *FGFR3* likley provides an explanation as to why FGFR3 signalling does not itself repress FGFR3 expression.

FGFR3 mutation is one of the most common oncogenes in transitional cell carcinomas of the bladder, also described at relatively high frequency in cervical cancer (1). Recent data has confirmed that *FGFR3* is also activated by translocations in cancer, that generate a fusion protein between *FGFR3* deleting the last exon of *FGFR3* and a number of partner proteins, in glioblastoma (38), bladder cancer(39), and upper aero-digestive tract squamous cancers (9). The clinical translational challenge in tackling the upregulation of receptor tyrosine kinases in resistance to targeted therapies is the identification of the receptor that drives resistance. Our data partially overcomes this challenge for *FGFR3* driven bladder cancer by demonstrating that EGFR is active and mediates resistance in all five *FGFR3* driven cell lines examined. The MET receptor has also been shown to be an important receptor mediating resistance, potentially through both paracrine stromal release (33) or autocrine production of HGF ligand (40). Our results are potentially conflicting with recent data that suggested MET as the mediator of resistance to FGFR3 targeting in RT112M (33, 40). However, we show that EGFR is the receptor that compensates for FGFR inhibition, and that this translates to substantial combination efficacy *in vivo* (Figure 7). Examining a publically available gene expression series we find that TGFα mRNA is expressed at high levels in bladder cancer (Figure 7D), along with expression of EGFR (Supplementary Figure 7A), whereas HGF mRNA is expressed at low levels (Supplementary Figure 7B), suggesting that our observations may be clinically relevant. Our data is also consistent with the recently identified role of EGFR in mediating resistance to mutant *BRAF* targeting in colon cancer (17, 34). However, our results do suggest caution in the combination of FGFR and EGFR inhibitors, with the combination of PD173074 and gefitinib poorly tolerated in mice at the doses used (Supplementary Figure 6). The combination of PD173074 and the EGFR inhibitory antibody cetuximab had improved tolerance (Supplementary Figure 6). In addition FGFR tyrosine kinase inhibitors typically broadly inhibit FGFR1/2/3, and the

Europe PMC Funders Author Manuscripts

increased specificity of FGFR3 therapeutic antibodies may potentially further mitigate toxicity (41, 42).

Our study illustrates the power of parallel RNA interference genetic screens to identify key determinants of resistance to targeted therapies. Through simultaneous examination of multiple cell lines with related oncogenic aberrations, the key common determinants of sensitivity can be identified, which may remain obscured by the multiplicity of effects and noise seen in any one individual screen (Supplementary Figure 1B). This approach could be applied to multiple different targeted therapies to identify the key determinants of sensitivity and reveal the common shared mechanisms of resistance.

Methods

Cell lines and antibodies

Bladder cells lines (RT112M, MGHU3, 639V, 97.7, 94.10) were from the laboratory of MA Knowles (13). Other cell lines were obtained from ATCC or Asterand. Cell lines were banked in multiple aliquots on receipt to reduce risk of phenotypic drift, and identity confirmed by STR profiling with the PowerPlex 1.2 System (Promega). Cell lines were maintained in phenol red free DMEM, DMEM/F12, or RPMI with 10% FBS (PAA gold) and 2mM L-glutamine (Sigma-Aldrich, Dorset, UK). Antibodies used were phosphorylated AKT-Ser473 (4058), AKT (4691), phospho-ERK1/2-Thr202/Tyr204 (4370), EGFR (2232), phospho-EGFR-tyr 1068 (3777), phospho-CDC25C-Thr48 (9527), phospho-SRC Y416 (2101), SRC (2109) (all Cell Signalling Technology, Danvers, MA), β-actin (A5441) (Sigma), FGFR3 (sc-13121), EGFR (sc-03), TGFα (sc-374433), p27 (sc-528), PARP (sc-7150), FRS2 (sc-8318) (Santa-Cruz Biotechnology, Santa Cruz, CA). PD173074 was from Sigma, gefitinib from Tocris, and CI-1040 from Selleckchem.

siRNA screening

Screening was in 384 well plates with a Dharmacon siGENOME SMARTpools library targeting all known protein kinases and phosphatases essentially as described previously (18, 43). Briefly, cells were reverse transfected at final siRNA concentration 20nM, at 48 hours post transfection half the plates were treated with PD173074 at the EC50 and half vehicle, and survival was assessed after 72 hours exposure with Cell Titre-Glo cell viability assay (Promega, Madison, WI). Individual plates were median normalised before combination. The siRNA library was supplemented with non-targeting siRNA, PLK1 siRNA as a viability control, and 4 individual siRNA against the FGFR1-4 receptor family (Supplementary Table 2 and Table 3). Screens were only accepted with a Z' factor >0.3.

To assess the effect of siRNA on growth/survival, the effect of siRNA in the vehicle plates was expressed as a Z score, with the standard deviation estimated from the median absolute deviation (MAD). A Z score of <-2, approximately the 95% confidence intervals, was considered evidence of a significant decrease in survival with siRNA.

To assess the effect of siRNA on sensitivity to PD173074 the log2 ratio between growth in PD173074 plates and vehicle plates was assessed and expressed as a Z score. A Z score of <-1.645 was considered evidence of increased sensitivity to PD170374, and >1.645 as relative resistance (cut-offs equivalent to putative 90% confidence intervals). A lower cut-off was used for sensitivity score to reflect that multiple siRNA altered sensitivity, affecting the null hypothesis in assessment of the standard deviation from the MAD, and clear evidence that reproducible effects were seen with siRNA using this cut-off (Supplementary Figure 1).

In vitro cell line assessment

Clonogenic assays were conduced in 6 well plates, with 1000-2000 cells seeded per well, and 24 hours later cells exposed to 500 nM PD173074, 250 nM Gefitinib, or the combination, followed by growth in media for 2 weeks to allow colony growth. Colonies were fixed, stained with sulforhodamine B, and counted. For short-term survival assays, cells were exposed to fixed-ratio combinations of PD173074 and gefitinib, and survival was assessed after 72 hours exposure with Cell Titre-Glo cell viability assay (Promega, Madison, WI). For EGFR siRNA short-term survival assays RT112M cells were reverse transfected at final siRNA concentration 20nM, at 48 hours post transfection plates were treated with PD173074 at the EC50 or vehicle, and survival was assessed after 72 hours exposure.

siRNA Data analysis

To compare siRNA results between two groups, we used supervised methods calculating the difference in the median effect of the siRNAs between the 2 groups, followed by estimation of a p value by permutation of labels to create a distribution for comparison with the actually differences (43). A significance cut-off of $p < 0.05$ was used.

Western blotting and FACS

Cell lines where grown on 35mm plates, treated as indicated, and lysed in NP40 lysis buffer. Western blots were carried out with precast TA or Bis-Tris gels (Invitrogen) as previously described. FACS analysis was performed as previously described (44).

Immunofluorescence

Cells grown on coverslips were fixed with 4% paraformaldehyde, before incubation with primary antibodies against EGFR (1:100, sc-03), FGFR3 (1:100, sc-13121) EEA1 (1:1000, sc-33585) (Santa-Cruz Biotechnology, Santa Cruz, CA), Alexa-488 phalloidin (1:1000, A12379) (Invitrogen), and corresponding secondary Alexa-444 or Alexa-555 conjugates antibodies, with DAPI nuclear stain. Cells were visualized with a Leica Confocal microscope.

Quantitative PCR

cDNA was synthesised from RNA using Superscript III and random hexamers (Invitrogen). Quantitative PCR was performed by absolute quantification with TAQMAN chemistry on an ABI Prism 7900T System (Applied Biosystems) with FGFR3 (Hs00997 400) expressed relative to control gene GAPDH (Hs 02758991). EGFR was sequenced with the cobas® EGFR Mutation Test (Roche Diagnostics).

Xenografts

RT112M xenografts in nude mice were generated by transplantation as previously described (13). In the first experiement mice were treated with PD173074 20mg/kg by intraperitoneal injection, gefitinib 100mg/kg by oral gavage, or the combination, for 3 days. In the second experiment mice were treated with PD173074 15mg/kg on days 0-3 and 7-10, cetuximab 40mg/kg day 0 day 3 day 7 and day 10 , or the combination by intraperitoneal injection. Tumour size was assessed at least three times a week. Time to tumour doubling was assessed by Kaplan-Meier methods as either doubling of relative tumour volume or tumour ulceration, censoring mice lost to follow-up through reasons not related to tumour progression. Experiments were performed under a UK Home Office Project License assessed by the University of Bradford ethical review committee.

Europe PMC Funders Author Manuscripts

Statistical analysis

All statistical tests were performed with GraphPad Prism version 5.0 or Microsoft Excel. Unless stated otherwise, p values were two tailed and considered significant if $p<0.05$. Error bars represent SEM of three experiments. Normalised gene expression data assessed on Affymetrix Human Genome U133A Arrays from Sanchez-Carbayo (45) et al were downloaded as log2 median centered data with probe 205016_at for TGFA from Oncomine (46)..

Supplementary Material

Refer to Web version on PubMed Central for supplementary material.

Acknowledgments

We thank Christopher Marshall for discussion and advice on the data. We thank David Gonzalez de Castro for performing EGFR sequencing.

Funding statement This work was supported by grants from Cancer Research UK C30746/A10038 and C347/A11847. Dr Nicholas Turner is a CRUK Clinician Scientist. We acknowledge NHS funding to the NIHR Biomedical Research Centre.

Financial support: M.H-A, A.A., N.T. were supported by Cancer Research UK grants C30746/A10038 and C347/A11847.

References

1. Cappellen D, De Oliveira C, Ricol D, de Medina S, Bourdin J, Sastre-Garau X, et al. Frequent activating mutations of FGFR3 in human bladder and cervix carcinomas. Nat Genet. 1999; 23:18–20. [PubMed: 10471491]
2. Pollock PM, Gartside MG, Dejeza LC, Powell MA, Mallon MA, Davies H, et al. Frequent activating FGFR2 mutations in endometrial carcinomas parallel germline mutations associated with craniosynostosis and skeletal dysplasia syndromes. Oncogene. 2007; 26:7158–62. [PubMed: 17525745]
3. Dutt A, Salvesen HB, Chen TH, Ramos AH, Onofrio RC, Hatton C, et al. Drug-sensitive FGFR2 mutations in endometrial carcinoma. Proc Natl Acad Sci U S A. 2008; 105:8713–7. [PubMed: 18552176]
4. Courjal F, Cuny M, Simony-Lafontaine J, Louason G, Speiser P, Zeillinger R, et al. Mapping of DNA amplifications at 15 chromosomal localizations in 1875 breast tumors: definition of phenotypic groups. Cancer Res. 1997; 57:4360–7. [PubMed: 9331099]
5. Weiss J, Sos ML, Seidel D, Peifer M, Zander T, Heuckmann JM, et al. Frequent and focal FGFR1 amplification associates with therapeutically tractable FGFR1 dependency in squamous cell lung cancer. Sci Transl Med. 2010; 2:62ra93.
6. Kunii K, Davis L, Gorenstein J, Hatch H, Yashiro M, Di Bacco A, et al. FGFR2-amplified gastric cancer cell lines require FGFR2 and Erbb3 signaling for growth and survival. Cancer Res. 2008; 68:2340–8. [PubMed: 18381441]
7. Heiskanen M, Kononen J, Barlund M, Torhorst J, Sauter G, Kallioniemi A, et al. CGH, cDNA and tissue microarray analyses implicate FGFR2 amplification in a small subset of breast tumors. Anal Cell Pathol. 2001; 22:229–34. [PubMed: 11564899]
8. Singh D, Chan JM, Zoppoli P, Niola F, Sullivan R, Castano A, et al. Transforming Fusions of FGFR and TACC Genes in Human Glioblastoma. Science. 2012
9. Wu YM, Su F, Kalyana-Sundaram S, Khazanov N, Ateeq B, Cao X, et al. Identification of Targetable FGFR Gene Fusions in Diverse Cancers. Cancer Discov. 2013
10. Turner N, Grose R. Fibroblast growth factor signalling: from development to cancer. Nat Rev Cancer. 2010; 10:116–29. [PubMed: 20094046]

11. Turner N, Lambros MB, Horlings HM, Pearson A, Sharpe R, Natrajan R, et al. Integrative molecular profiling of triple negative breast cancers identifies amplicon drivers and potential therapeutic targets. Oncogene. 2010; 29:2013–23. [PubMed: 20101236]
12. Tannheimer SL, Rehemtulla A, Ethier SP. Characterization of fibroblast growth factor receptor 2 overexpression in the human breast cancer cell line SUM-52PE. Breast Cancer Res. 2000; 2:311–20. [PubMed: 11056689]
13. Lamont FR, Tomlinson DC, Cooper PA, Shnyder SD, Chester JD, Knowles MA. Small molecule FGF receptor inhibitors block FGFR-dependent urothelial carcinoma growth in vitro and in vivo. Br J Cancer. 2011; 104:75–82. [PubMed: 21119661]
14. Andre F, Bachelot TD, Campone M, Dalenc F, Perez-Garcia JM, Hurvitz SA, et al. A multicenter, open-label phase II trial of dovitinib, an FGFR1 inhibitor, in FGFR1 amplified and non-amplified metastatic breast cancer. J Clin Oncol. 2012; 29
15. Soria JC, Dienstmann R, de Braud F, Cereda R, Bahleda R, Hollebecque A, et al. FIRST-IN-MAN STUDY OF E-3810, A NOVEL VEGFR AND FGFR INHIBITOR, IN PATIENTS WITH ADVANCED SOLID TUMORS. Annals of Oncology. 2012; 23:L2.5.
16. Berns K, Horlings HM, Hennessy BT, Madiredjo M, Hijmans EM, Beelen K, et al. A functional genetic approach identifies the PI3K pathway as a major determinant of trastuzumab resistance in breast cancer. Cancer Cell. 2007; 12:395–402. [PubMed: 17936563]
17. Prahallad A, Sun C, Huang S, Di Nicolantonio F, Salazar R, Zecchin D, et al. Unresponsiveness of colon cancer to BRAF(V600E) inhibition through feedback activation of EGFR. Nature. 2012; 483:100–3. [PubMed: 22281684]
18. Turner NC, Lord CJ, Iorns E, Brough R, Swift S, Elliott R, et al. A synthetic lethal siRNA screen identifying genes mediating sensitivity to a PARP inhibitor. EMBO J. 2008; 27:1368–77. [PubMed: 18388863]
19. Avraham R, Yarden Y. Feedback regulation of EGFR signalling: decision making by early and delayed loops. Nat Rev Mol Cell Biol. 2011; 12:104–17. [PubMed: 21252999]
20. Wang Z, Wang M, Lazo JS, Carr BI. Identification of epidermal growth factor receptor as a target of Cdc25A protein phosphatase. J Biol Chem. 2002; 277:19470–5. [PubMed: 11912208]
21. Wang R, He G, Nelman-Gonzalez M, Ashorn CL, Gallick GE, Stukenberg PT, et al. Regulation of Cdc25C by ERK-MAP kinases during the G2/M transition. Cell. 2007; 128:1119–32. [PubMed: 17382881]
22. Naski MC, Wang Q, Xu J, Ornitz DM. Graded activation of fibroblast growth factor receptor 3 by mutations causing achondroplasia and thanatophoric dysplasia. Nat Genet. 1996; 13:233–7. [PubMed: 8640234]
23. Rousseau F, el Ghouzzi V, Delezoide AL, Legeai-Mallet L, Le Merrer M, Munnich A, et al. Missense FGFR3 mutations create cysteine residues in thanatophoric dwarfism type I (TD1). Hum Mol Genet. 1996; 5:509–12. [PubMed: 8845844]
24. di Martino E, L'Hote CG, Kennedy W, Tomlinson DC, Knowles MA. Mutant fibroblast growth factor receptor 3 induces intracellular signaling and cellular transformation in a cell type- and mutation-specific manner. Oncogene. 2009; 28:4306–16. [PubMed: 19749790]
25. Chandarlapaty S, Sawai A, Scaltriti M, Rodrik-Outmezguine V, Grbovic-Huezo O, Serra V, et al. AKT inhibition relieves feedback suppression of receptor tyrosine kinase expression and activity. Cancer Cell. 2011; 19:58–71. [PubMed: 21215704]
26. Serra V, Scaltriti M, Prudkin L, Eichhorn PJ, Ibrahim YH, Chandarlapaty S, et al. PI3K inhibition results in enhanced HER signaling and acquired ERK dependency in HER2-overexpressing breast cancer. Oncogene. 2011; 30:2547–57. [PubMed: 21278786]
27. Karaman MW, Herrgard S, Treiber DK, Gallant P, Atteridge CE, Campbell BT, et al. A quantitative analysis of kinase inhibitor selectivity. Nat Biotechnol. 2008; 26:127–32. [PubMed: 18183025]
28. Oneyama C, Ikeda J, Okuzaki D, Suzuki K, Kanou T, Shintani Y, et al. MicroRNA-mediated downregulation of mTOR/FGFR3 controls tumor growth induced by Src-related oncogenic pathways. Oncogene. 2011; 30:3489–501. [PubMed: 21383697]

Europe PMC Funders Author Manuscripts

29. Parker BC, Annala MJ, Cogdell DE, Granberg KJ, Sun Y, Ji P, et al. The tumorigenic FGFR3-TACC3 gene fusion escapes miR-99a regulation in glioblastoma. J Clin Invest. 2013; 123:855–65. [PubMed: 23298836]
30. Catto JW, Miah S, Owen HC, Bryant H, Myers K, Dudziec E, et al. Distinct microRNA alterations characterize high- and low-grade bladder cancer. Cancer Res. 2009; 69:8472–81. [PubMed: 19843843]
31. Ishizawar R, Parsons SJ. c-Src and cooperating partners in human cancer. Cancer Cell. 2004; 6:209–14. [PubMed: 15380511]
32. Bromann PA, Korkaya H, Courtneidge SA. The interplay between Src family kinases and receptor tyrosine kinases. Oncogene. 2004; 23:7957–68. [PubMed: 15489913]
33. Wilson TR, Fridlyand J, Yan Y, Penuel E, Burton L, Chan E, et al. Widespread potential for growth-factor-driven resistance to anticancer kinase inhibitors. Nature. 2012; 487:505–9. [PubMed: 22763448]
34. Corcoran RB, Ebi H, Turke AB, Coffee EM, Nishino M, Cogdill AP, et al. EGFR-mediated re-activation of MAPK signaling contributes to insensitivity of BRAF mutant colorectal cancers to RAF inhibition with vemurafenib. Cancer Discov. 2012; 2:227–35. [PubMed: 22448344]
35. Garofalo M, Romano G, Di Leva G, Nuovo G, Jeon YJ, Ngankeu A, et al. EGFR and MET receptor tyrosine kinase-altered microRNA expression induces tumorigenesis and gefitinib resistance in lung cancers. Nat Med. 2011; 18:74–82. [PubMed: 22157681]
36. Straussman R, Morikawa T, Shee K, Barzily-Rokni M, Qian ZR, Du J, et al. Tumour micro-environment elicits innate resistance to RAF inhibitors through HGF secretion. Nature. 2012; 487:500–4. [PubMed: 22763439]
37. Wang W, Eddy R, Condeelis J. The cofilin pathway in breast cancer invasion and metastasis. Nat Rev Cancer. 2007; 7:429–40. [PubMed: 17522712]
38. Singh D, Chan JM, Zoppoli P, Niola F, Sullivan R, Castano A, et al. Transforming fusions of FGFR and TACC genes in human glioblastoma. Science. 2012; 337:1231–5. [PubMed: 22837387]
39. Williams SV, Hurst CD, Knowles MA. Oncogenic FGFR3 gene fusions in bladder cancer. Hum Mol Genet. 2012
40. Harbinski F, Craig VJ, Sanghavi S, Jeffery D, Liu L, Sheppard KA, et al. Rescue screens with secreted proteins reveal compensatory potential of receptor tyrosine kinases in driving cancer growth. Cancer Discov. 2012; 2:948–59. [PubMed: 22874768]
41. Qing J, Du X, Chen Y, Chan P, Li H, Wu P, et al. Antibody-based targeting of FGFR3 in bladder carcinoma and t(4;14)-positive multiple myeloma in mice. J Clin Invest. 2009; 119:1216–29. [PubMed: 19381019]
42. Trudel S, Stewart AK, Rom E, Wei E, Li ZH, Kotzer S, et al. The inhibitory anti-FGFR3 antibody, PRO-001, is cytotoxic to t(4;14) multiple myeloma cells. Blood. 2006; 107:4039–46. [PubMed: 16467200]
43. Brough R, Frankum JR, Sims D, Mackay A, Mendes-Pereira AM, Bajrami I, et al. Functional viability profiles of breast cancer. Cancer Discov. 2011; 1:260–73. [PubMed: 21984977]
44. Turner N, Pearson A, Sharpe R, Lambros M, Geyer F, Lopez-Garcia MA, et al. FGFR1 amplification drives endocrine therapy resistance and is a therapeutic target in breast cancer. Cancer Res. 2010; 70:2085–94. [PubMed: 20179196]
45. Sanchez-Carbayo M, Socci ND, Lozano J, Saint F, Cordon-Cardo C. Defining molecular profiles of poor outcome in patients with invasive bladder cancer using oligonucleotide microarrays. J Clin Oncol. 2006; 24:778–89. [PubMed: 16432078]
46. Rhodes DR, Yu J, Shanker K, Deshpande N, Varambally R, Ghosh D, et al. ONCOMINE: a cancer microarray database and integrated data-mining platform. Neoplasia. 2004; 6:1–6. [PubMed: 15068665]

Europe PMC Funders Author Manuscripts

Statement of Significance

Our data identifies a novel therapeutic approach to the treatment of *FGFR3* mutant cancer, emphasising the potential of combination approaches targeting both FGFR3 and EGFR. Our data extends the role of EGFR in mediating resistance to inhibitors targeting a mutant oncogene, demonstrating that EGFR signalling can repress mutant *FGFR3* to induce intrinsic resistance to FGFR targeting.

Europe PMC Funders Author Manuscripts

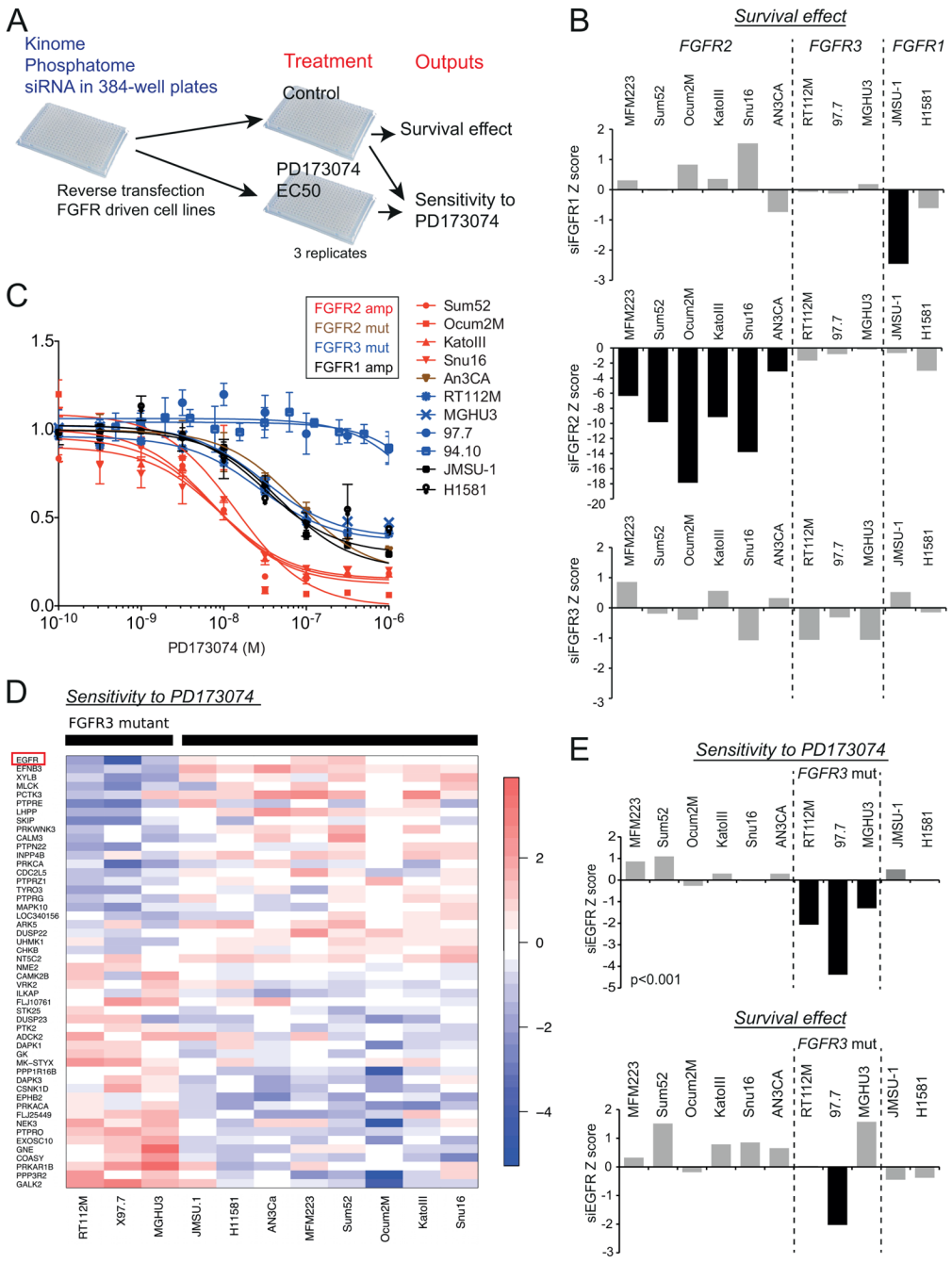

Figure 1. High-throughput siRNA Kinome/Phosphatome to identify genes required for the growth of *FGFR* amplified and mutant cell lines and sensitivity to FGFR inhibition

A. Schematic of siRNA screen. Cells were reverse transfected in 384 well plates with siRNA SMARTpools targeting all known protein kinases and phosphatases, and 48 hours later exposed to PD170374 at EC50, or control, and survival assessed after 72 hours exposure. The effect of siRNA on survival was assessed on the vehicle plates (Survival effect), and the effect of siRNA on sensitivity to PD173074 was assessed as the relative growth in PD173074 plates compared to vehicle (Sensitivity to PD173074). Both analyses were expressed as a Z score.

B. Survival effect of FGFR1, FGFR2, and FGFR3 siRNA according to *FGFR* gene mutation/amplification; left *FGFR1* amplified, centre *FGFR3* mutation, right *FGFR2* amplified and mutated (AN3CA). Black bars indicate those siRNA with a significant effect in cell survival, defined as a Z score <-2.
C. Relative growth of the panel of screened cell lines to a range of concentration of PD173074.
D. Supervised clustering of the siRNA effect on sensitivity to PD173074, with the differential effect of siRNA according to *FGFR3* mutational status. Displayed are siRNA with a permutation p value <0.05 ordered by mean effect in the *FGFR3* activated cell lines.
E. *Top.* EGFR siRNA increased sensitivity to PD173074 specifically in *FGFR3* activated cell lines, p=0.001 Student's T test. *Bottom.* Survival effect of EGFR siRNA. EGFR siRNA significantly reduced the survival of the 97-7 cell line.

Europe PMC Funders Author Manuscripts

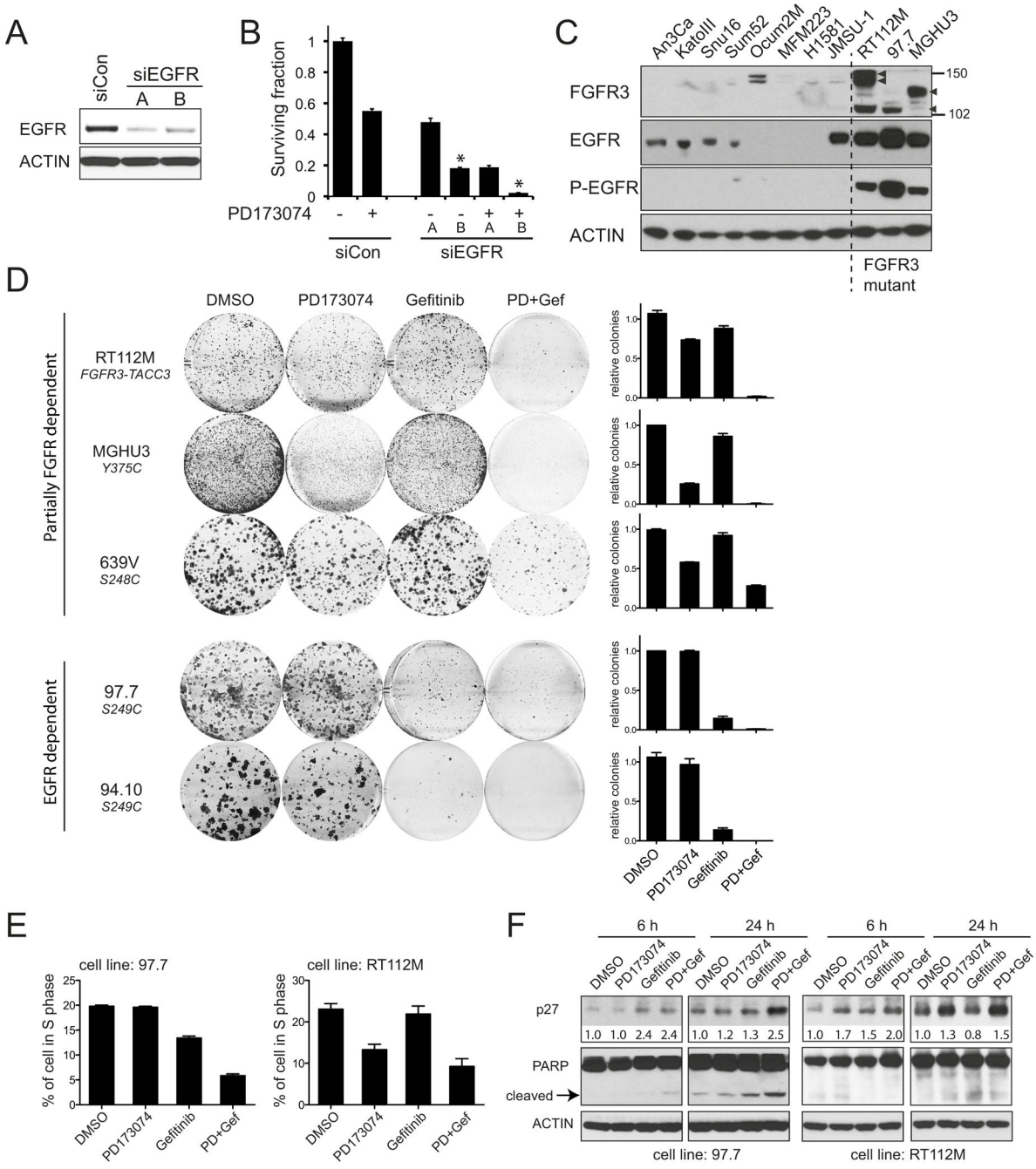

Figure 2. EGFR is intrinsically active in *FGFR3* activated lines with combination efficacy from targeting both EGFR and FGFR3

A. Western blots of RT112M cells transfected 72 hours earlier with siCON or individual siRNA targeting EGFR (siEGFR-A/B).

B. Growth of RT112M transfected with siCON and two individual siRNA targeting EGFR (A / B) and 48 hours post transfection exposed to a fixed dose of PD173074 (+) or vehicle (-) for 72 hours.

C. Western blot of indicated cell lystates blotted for FGFR3, EGFR, and phosphorylated EGFR, with actin loading control. The three FGFR3 activated cell lines are indicated.

Europe PMC Funders Author Manuscripts

D. Clonogenic survival assays in indicated cell lines treated continuously with 500nM PD173074, 250nM gefitinib, the combination, or vehicle alone. Activating aberration in *FGFR3* is indicated for each cell line, with cell lines classified as either partially FGFR3 dependent or primarily EGFR dependent. (*Right*) quantification of three independent experiments.

E. Analysis of S phase fraction from propidium iodidie FACS profiles of indicated cell lines treated for 24 hours with 500nM PD173074, 250nM gefitinib, combination, or vehicle. * $p<0.05$ Student's T test.

F. Expression of p27 increases with combination therapy at 24 hours, with a minor increase in cleaved PARP in 97-7 cells.

Europe PMC Funders Author Manuscripts

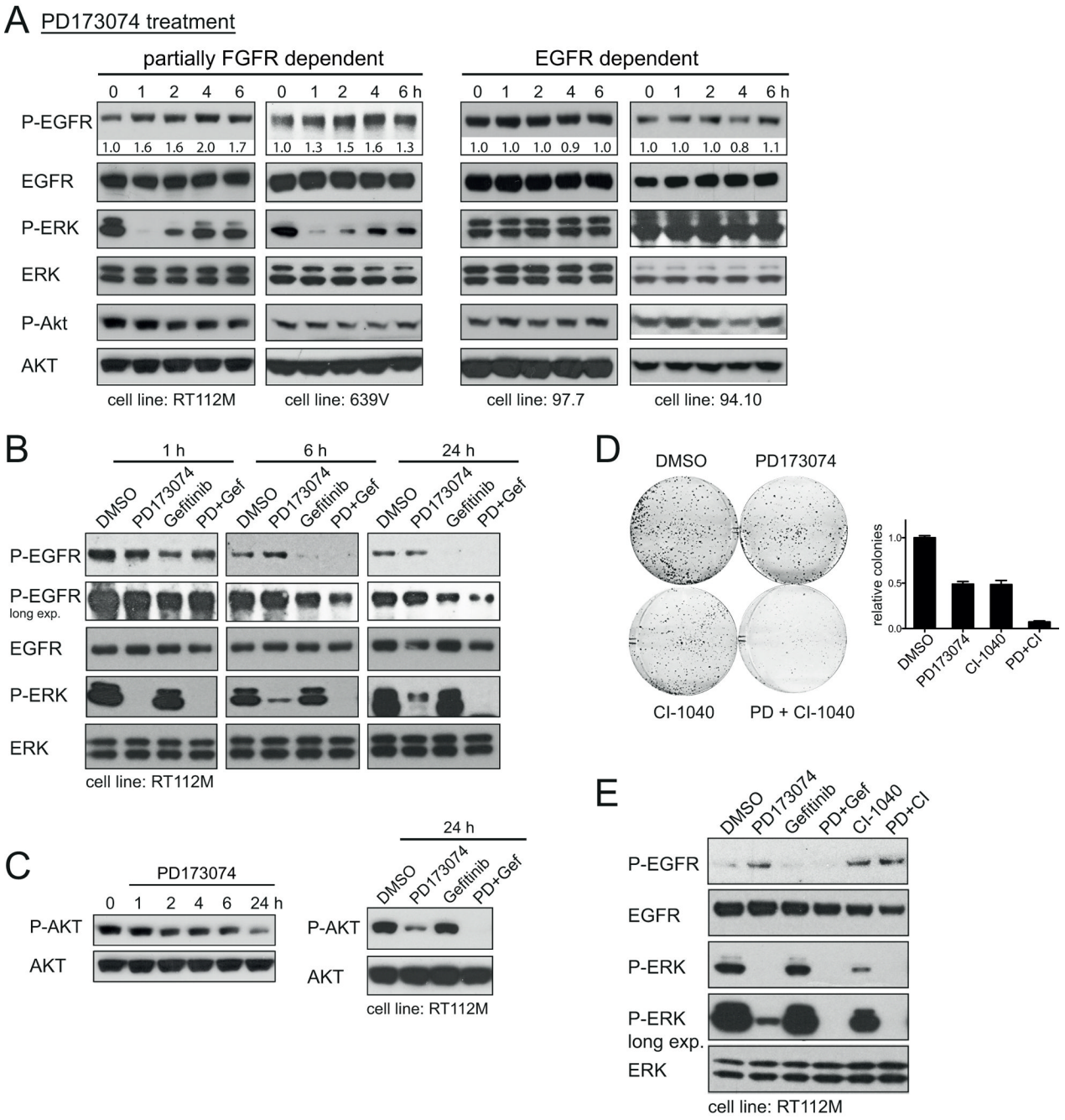

Figure 3. EGFR signalling is upregulated in response to FGFR3 inhibition in partially FGFR dependent cell lines

A. Western blot of FGFR3 dependent (RT112M and 639V) and EGFR dependent (97.7 and 94.10) cell lysates treated for the indicated times with 500nM PD173074 blotted for phosphorylated and total EGFR, ERK1/2 and AKT Ser 473.

B. Western blot of RT112M cell lysates treated for the indicated times with 500nM PD173074, 250 nM gefitinib, combination, or vehicle, blotted for phosphorylated and total EGFR and ERK1/2.

C. Western blot of serine 473 phosphorylated and total AKT in RT112M cells treated as indicated.

Europe PMC Funders Author Manuscripts

D. Clonogenic survival assay of RT112M cells with PD173074 500nM, MEK inhibitor CI-1040 100nM, or the combination. *Right*: quantification of three independent experiments. E. Western blot of RT112M cells treated with PD173074, gefitinib, or CI-1040 100nM as indicated for 6 hours.

Europe PMC Funders Author Manuscripts

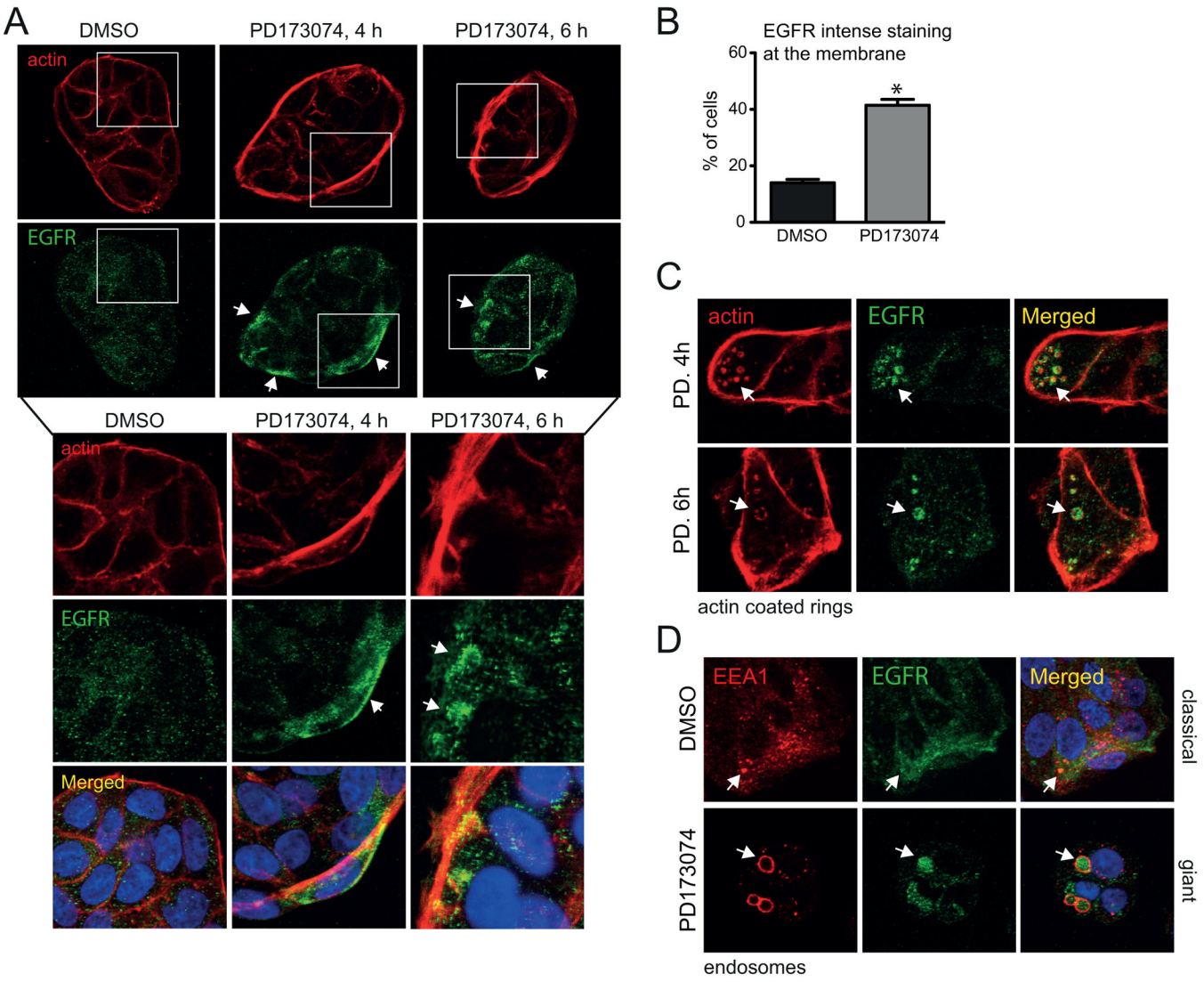

Figure 4. Localisation of EGFR in response to FGFR inhibition in partially FGFR3 dependent cell lines

A., Immunofluoresence of RT112M cells treated with 500nM PD170374 for indicated times, or DMSO vehicle, stained for F-actin (red) and EGFR (green).

B. Quantification of three independent immunofluoresence experiments of RT112M cells treated with 500nM PD173074 for 4 hours, proportion of cells with EGFR membrane staining. * P<0.001 Student's t test.

C. and D. Immunofluoresence of RT112M cells treated with 500nM PD170374 for 4 or 6 hours. C. Stained for actin (red) and EGFR (green) and D. at 4 hours stained for EEA1 (red) and EGFR (green).

Europe PMC Funders Author Manuscripts

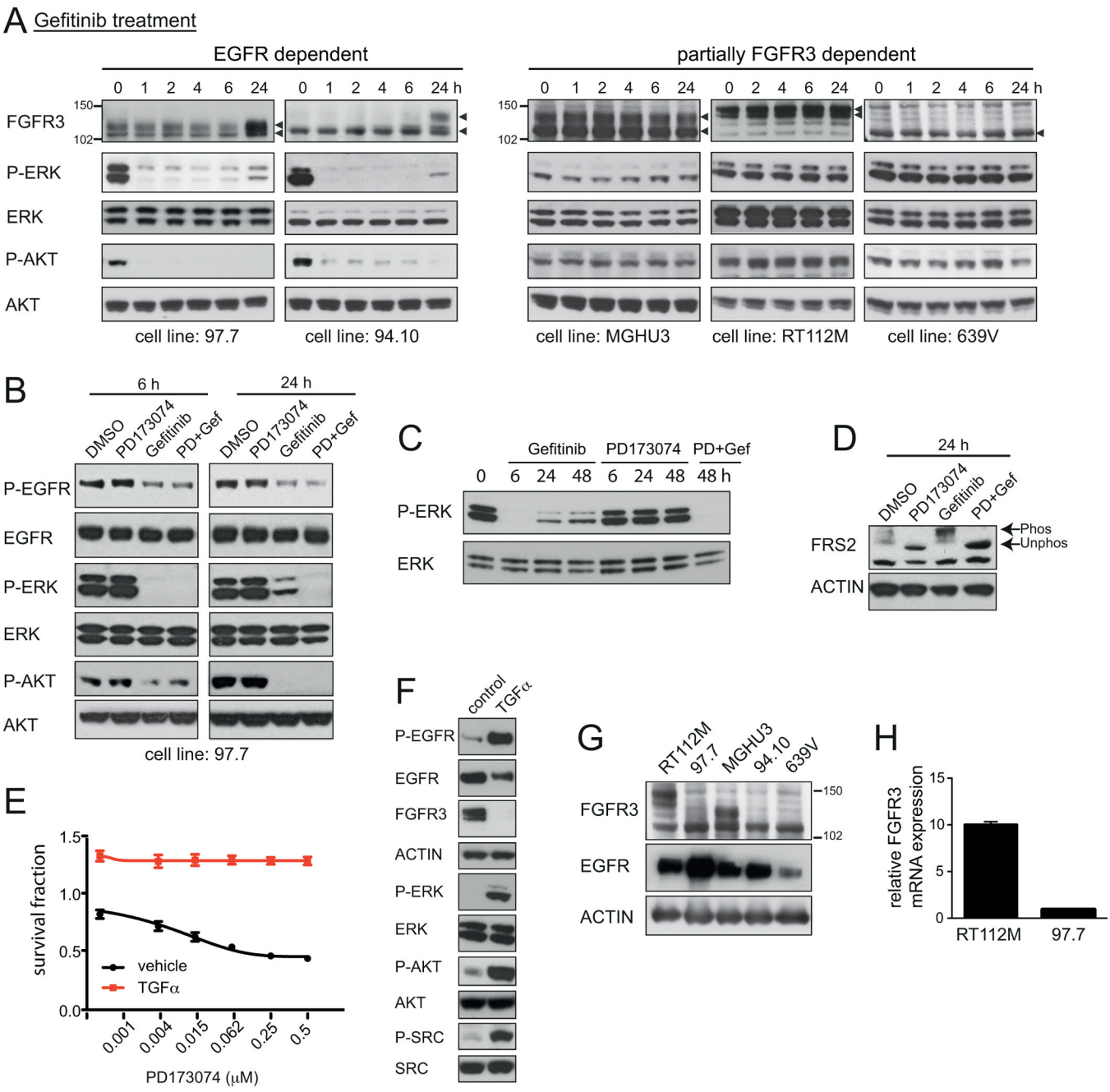

Figure 5. EGFR mediates intrinsic resistance to FGFR3 targeting through repression of FGFR3 expression, with delayed upregulation of FGFR3 expression in response to EGFR inhibiton

A. Western blot of partially FGFR3 dependent cell lines (MGHU3, RT112M, 639V) and EGFR dependent cell line (97-7, 94-10) lysates treated for the indicated times with gefitinib.

B and C. Western blot of 97.7 cell lysates treated for the indicated times with PD173074, gefitinib, combination, or vehicle.

D. Western blot of FRS2 following treatment with PD173074, gefitinib or the combination.

E. RT112M cells grown for 72 hours in increasing concentrations of PD173074 in the presence of TGFα 10ng/ml or vehicle. Partially FGFR dependent RT112M acquire resistance to PD173074 in the presence of TGFα.

F. Western blot of RT112M lysates after 24 hours exposure to TGFα 10ng/ml or vehicle, blotted with indicated antibodies.
G. Western blot of cell lystates from *FGFR3* activated cell lines blotted for FGFR3, EGFR, and actin loading control.
H. Quantitative real time RT-PCR assessment FGFR3 mRNA expression in RT112M and 97.7 cell lines.

Europe PMC Funders Author Manuscripts

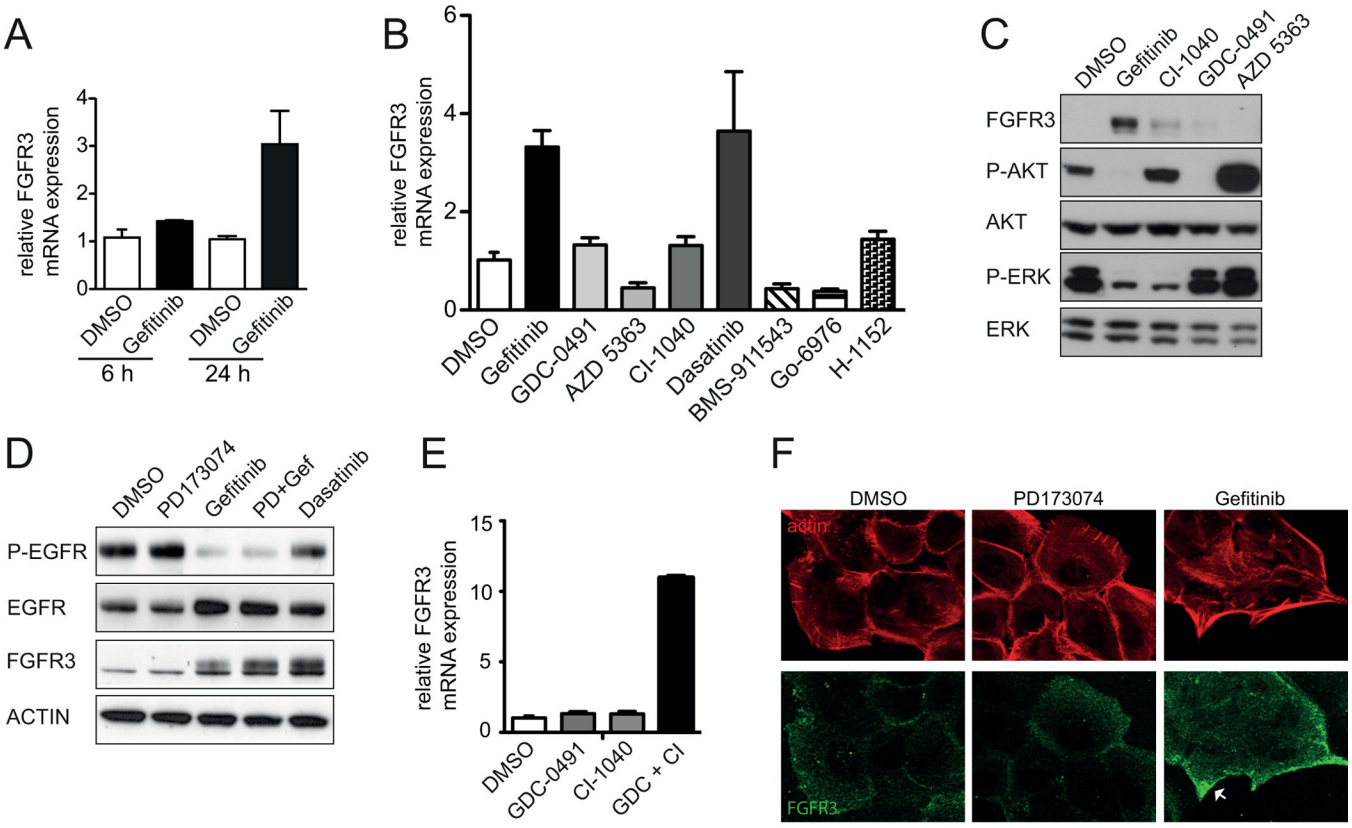

Figure 6. EGFR signalling regulates FGFR3 expression in part through SRC family signalling and the effects of multiple down-stream signal transduction pathways

A. 97-7 cells were treated with 6 or 24 hours with gefitinib, or DMSO, with quantitative real time RT-PCR assessment of *FGFR3* mRNA expressed relative to the level in DMSO treated cells.

B. 97-7 cells were treated for 24 hours with DMSO vehicle, 250nM gefitinib (EGFR inhibitor), 250nM GDC-0491 (PI3 kinase inhibitor), 200nM AZD5363 (AKT inhibitor), 500nM CI-1040 (MEK inhibitor), 100nM Dasatinib (SRC family inhibitor), 1μM BMS-911543 (JAK2 inhibitor), 100nM Go-6976 (Protein kinase C inhibitor), or 150nM H1152 (ROCK inhibitor). FGFR3 mRNA was assessed by quantitative real time RT-PCR relative to GAPDH, and expressed relative to DMSO treated cells.

C. and D. Western blot of 97-7 lysates after 24 hours exposure to indicated compounds, or a combination of gefitinib and PD173074, blotted with indicated antibodies.

E. 97-7 cells were treated for 24 hours with DMSO vehicle, 250nM GDC-0491, 500nM CI-1040, or the combination. FGFR3 mRNA was assessed by quantitative real time RT-PCR.

F. Immunofluoresence of 97-7 cells treated with PD170374 or gefitinib for 24 hours stained for actin (red) and FGFR3 (green)

Europe PMC Funders Author Manuscripts

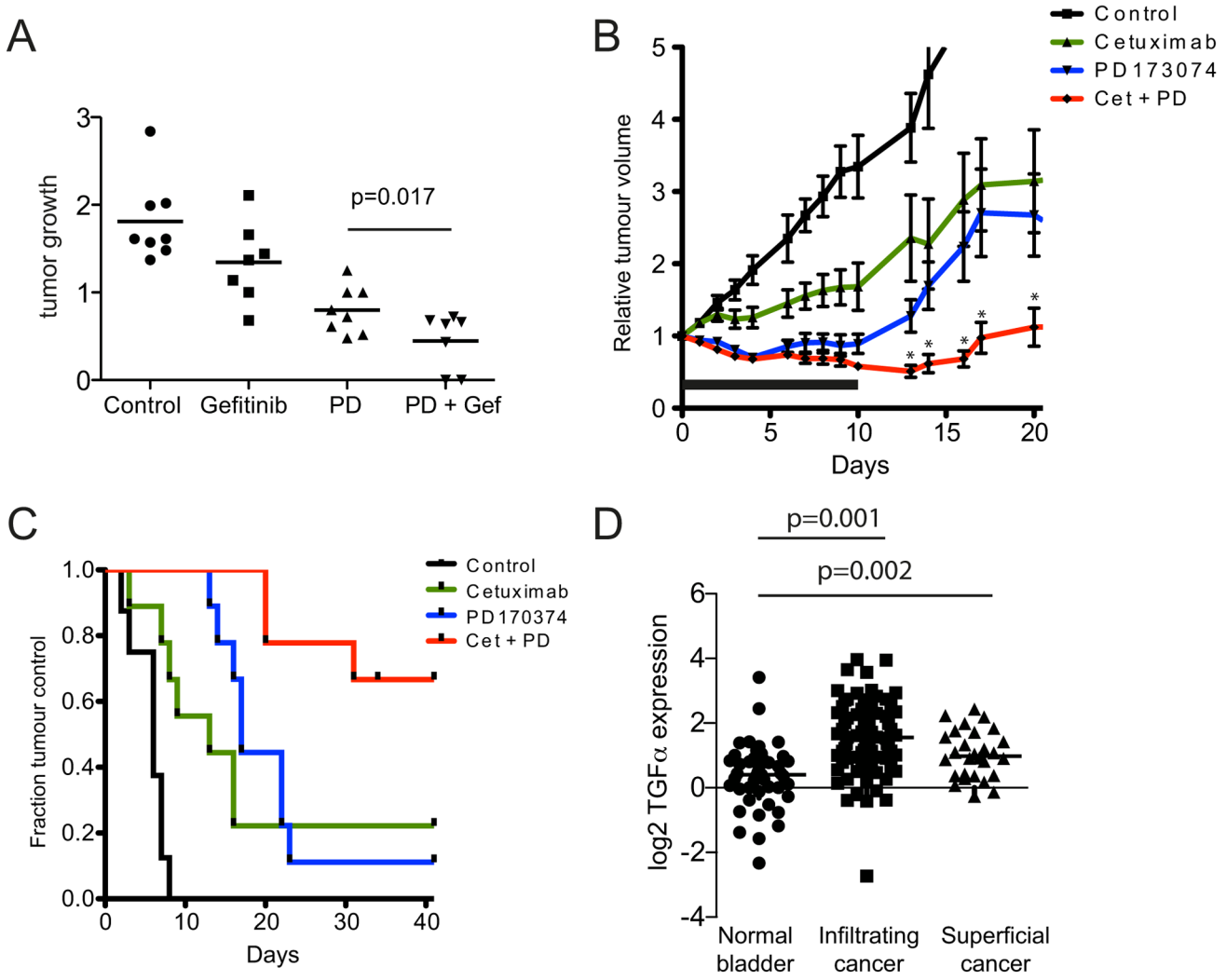

Figure 7. Inhibition of EGFR and FGFR3 has combination efficacy *in vivo*

A. RT112M xenografts were established in nude mice, and divided randomly into 4 groups treated with vehicle, PD173074 20mg/mg IP, gefitinib 110mg/kg PO, or combination of both inhibitors for 3 days. Tumour growth was assessed 7 days following commencement of therapy. Comparison between groups with Student's T test.

B. RT112M xenografts were established in nude mice, and divided randomly into 4 groups treated with vehicle, PD173074 15mg/mg IP (days 0-3 and days 7-10), cetuximab 40mg/kg IP (days 0,3,7,10) or combination of both inhibitors with solid bar indicating two week treatment interval. *p<0.01 compared to all other groups Student's T test.

C. Kaplan Meier plot of time to tumour doubling from experiment described in part B. Combination treated animals have substantially increased tumour control, p<0.01 Log Rank test comparing combination treated animals with all other groups.

D. Expression of TGFα mRNA in a publically available gene expression data set of normal bladder, invasive bladder cancers, and superficial type bladder cancers. Comparison between groups with Students T test.